Met. Mater. Int., Vol. 22, No. 2 (2016), pp. 288~294
doi: 10.1007/s12540-016-5487-x

Electron Back-Scattered Diffraction and Nanoindentation Analysis of Nanostructured Al Tubes Processed by Multipass Tubular-Channel Angular Pressing

Mohsen Mesbah[1,2], Ghader Faraji[3,*], and A. R. Bushroa[1,2]

[1]Department of Mechanical Engineering, Faculty of Engineering, University of Malaya, 50603 Kuala Lumpur, Malaysia
[2]Centre of Advanced Manufacturing and Material Processing (AMMP), Faculty of Engineering, University of Malaya, 50603 Kuala Lumpur, Malaysia
[3]School of Mechanical Engineering, College of Engineering, University of Tehran, Tehran, 11155-4563, Iran

(received date: 8 September 2015 / accepted date: 23 October 2015)

Microstructural evolution and mechanical properties of nanostructured 1060 aluminum alloy tubes processed by tubular-channel angular pressing (TCAP) process were investigated using electron back-scattered diffraction (EBSD), transmission electron microscopy (TEM) and nanoindentation analyzes. EBSD scans revealed a homogeneous ultrafine grained microstructure after the third passes of the TCAP process. Apart from that the mean grain sizes of the TCAP processed tubes were refined to 566 nm, 500 nm and 480 nm respectively after the first, second and third passes. The results showed that after the three TCAP passes, the grain boundaries with a high angle comprised 78% of all the boundaries. This is in comparison to the first pass processed sample that includes approximately 20% HAGBs. The TEM inspection afforded an appreciation of the role of very low-angle misorientation boundaries in the process of refining microstructure. Nanoindentation results showed that hardness was the smallest form of an unprocessed sample while the largest form of the processed sample after the three passes of TCAP indicated the highest resistant of the material. In addition, the module of elasticity of the TCAP processed samples was greater from that of the unprocessed sample.

Keywords: severe plastic deformation, transmission electron microscopy, electron backscattering diffraction (EBSD), grain refinement, nanostructured materials

1. INTRODUCTION

Aluminum and its alloys are desirable for use in different industries especially in the aerospace and automotive industry due to its lower density and high strength to weight. It should be noted though that commercially, pure Al does not have the required strength for some applications [1]. Severe plastic deformation (SPD) has been performed on the grain refinement to reduce this weakness [2-5]. The yield stress of 200 MPa has been achieved by (ECAP) [4]. Yadav and Bauri [6] processed the commercially pure aluminum (99.2%) using the friction stir processing (FSP) method. They reported that the yield stress of the friction stir processed (FSP) material improved by a factor of about 2.4 compared to the base material. The UTS also increased by 25% from 72 to 90 MPa [6]. Arzaghi *et al*. [7] used high pressure tube twisting (HPTT) to produce UFG pure aluminum 1050 with a grain size of about 300 nm up to a shear strain of 24. They also reported a remarkable improvement in the mechanical properties of the product. Faraji *et al*. developed the TCAP process to cause intense plastic strain in the tubular material without altering the cross-sectional area [8]. The tube was pressed into the die channel a number of times; the same strain was multiplied each time as a function of die parameters [8]. The texture evolution in TCAP materials has been studied before [9-11], but to this point there is virtually no study to investigate the texture evolution in TCAP materials by using the EBSD technique. Additionally, the nanomechanical response of these materials has yet to be explored. The present study aimed at investigating the quantitative characterization of the grains evolutions in commercially pure Al 1060 processed using the TCAP method, employing the EBSD and TEM techniques. Nanoindentation analysis was also used for mechanical characterization.

*Corresponding author: ghfaraji@ut.ac.ir

2. EXPERIMENTAL PROCEDURE

2.1. TCAP Principle

Figure 1(a) demonstrates the TCAP procedure. A hollow

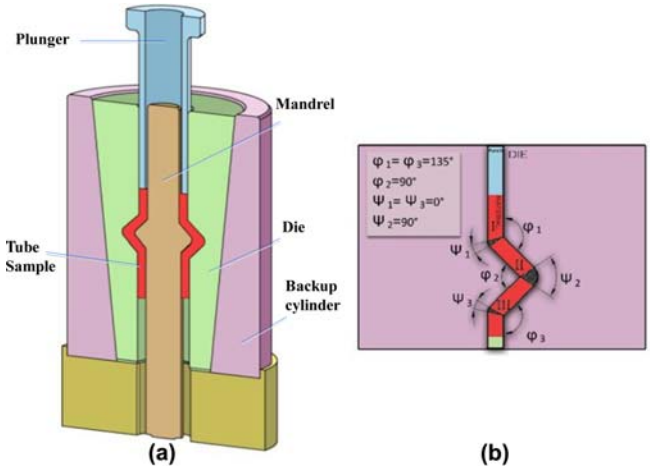

Fig. 1. (a) Illustration of TCAP and (b) related parameters of the die.

cylindrical punch was used to press the tube into a crevice in the middle of the die and mandrel that form a tubular angular channel with three shear zones I, II and III. The cross section of the tube remained constant before and after the process. In multi-pass TCAP, the procedure was repeated to develop unique strains without a decrease in the cross area of the workpiece. The TCAP facility comprised of a die and mandrel with three intersecting channels, a plunger, and a hydraulic press. The die and the plunger were made from tool steel and were heat treated to achieve a Rockwell hardness of 55 HRc. Before pressing, the tubes and plunger were lubricated using MoS_2 [12]. The TCAP processing was conducted at room temperature. The die geometry shown in Fig. 1(b) resulted in a strain of ~2.2 after each separate pass.

2.2. Materials

In this study, commercial purity 1060 Al with 99.6% purity in the form of as-cast ingots was used. Cylindrical samples with an outer diameter of 20 mm, a thickness of 2.5 mm and a length of 40 mm were formed by machining. Next, the samples were annealed at 350 ˚C for 2 h to attain a homogeneous and recrystallized microstructure.

2.3. Electron backscattered diffraction (EBSD)

The extruded tubular samples were cut perpendicular according to the direction of the extrusion for microstructural observations. Following TCAP, samples with a thickness of about 7 mm were cut from the centers of the samples one, two and three passes, vertical to the direction of the extrusion. The scanning parameters of EBSD were set so that a grain boundary was identified when the misorientation between 2 neighboring measurement points was more than 2°. Therefore, no grain boundary was seen with a misorientation less than 2°. Microstructural investigations were conducted using Oxford EBSD Instruments. Nordlys Nano from Oxford Instruments EBSD detector, which was attached to FIB-SEM Helios 600i from FEI. 20 kV and 1.4 nA electron beam were used for the measurements. A flat surface without native oxide was prepared by Polishing and FIB (Helios 600i from FEI). The mirror-like surface was obtained by polishing with 40 nm colloidal silica suspension. After polishing, Focus Ion Beam with 30 kV and 0.79 nA was scanned over the surface to eliminate native oxide that blocked the EBSD signals. The EBSD analysis was carried out using the TSL OIM software. A step size of 0.07–0.4 μm was used to carry out the EBSD acquisitions, the range of which was reduced from the non-deformed material to the material exposed to extreme deformation. For the EBSD mapping, the scan area of 20 μm×20 μm was chosen. Texture analyses were carried out by recording the pole figures of (111), (101) and (100) for all the differently deformed samples. When the misorientation between the neighboring measurement points was greater than 15°, a high angle grain boundary (HAGB) was identified.

2.4. Transmission electron microscopy (TEM)

To investigate the microstructure, the tubular samples were cut in a direction perpendicular to the extrusion direction. The Lamella Samples for TEM analysis were taken at the area along the middle of the tubes' thickness. Then, they were prepared using a twin jet polishing technique in a mixture of 30% nitric acid and 70% carbinol at minus 30 ˚C. Microstructural investigations were fulfilled by the TEM machine model FEI Tecnai TF20 at an accelerating voltage of 200 KV.

2.5. Nanoindentation

The nanoindentation experiment was performed by a Tribo indenter 750 Ubi system (Hysitron Inc., USA) using a Berkovich indenter on TCAP processed samples at a different number of passes. The indenter was penetrated into the specimens with a maximum normal load of 2000 μN. The speed for each loading and unloading step was also kept constant. However, the loading, holding and unloading times were set at 30 s, 10 s and 30 s, respectively. The electromagnetic force was used to press a Berkovich indenter against a sample (Standard type: 115° triangular pyramid). The depth of indentation is automatically assessed when the indenter is pressed against the sample.

3. RESULTS AND DISCUSSION

The EBSD/orientation imaging microscopy (OIM) patterns of the TCAP processed Al samples after 0, 1, 2, and 3 passes are shown in Fig. 2. The color maps presented in Fig. 2(a)-(d) indicate that the crystallographic orientation of the grains is parallel to the extrusion direction consistent with the key stereographic triangle presented in Fig. 2(i). Figures 2(e)-2(h) displays the corresponding grain boundary maps wherein the high angle grain boundaries (HAGBs) (i.e. the boundaries which have a relative misorientation

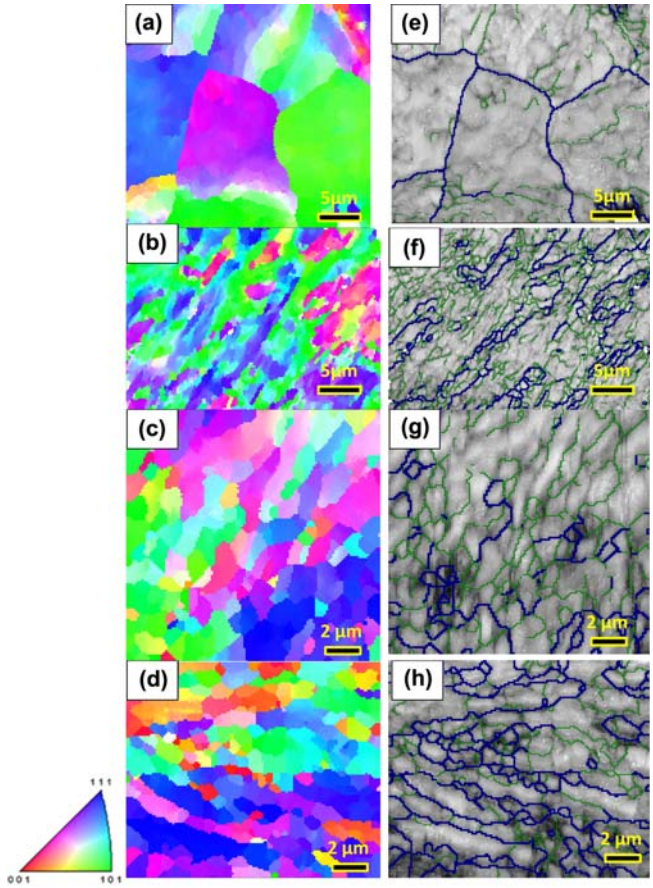

Fig. 2. EBSD maps obtained from the center region of the TCAP samples subjected to 0, 1, 2, and 3 passes. (a–d) Color maps and (e–h) boundary maps.(i) Representation of the color code used to identify the crystallographic orientations on a standard stereographic projection (red: (0 0 1); blue: (1 1 1); green: (1 0 1)).

larger than 15°) are shown as blue lines, and the small angle grain boundaries (i.e. those boundaries which have a relative misorientation from 2° to 15°) are shown as green lines. Misorientations and boundaries less than 2° are not considered in the maps due to the inaccuracy in the EBSD measurements [13]. An elongated grain microstructure are observed in the EBSD map along the TCAP induced shear bands. In addition, several subgrains are evident in the grains' interior structure, which are mostly oriented along the shear direction, building a 45° angle with the PD.

Figures 2(a) and 2(e) show the microstructure of an unprocessed Al tube. As can be seen, the size of the grains is relatively big by a mean grain size of approximately 75 μm. The microstructures shown in Figs. 2(b) and 2(f) indicate a strong texture at most locations. It demonstrates that most microstructure after one TCAP pass which comprises of both elongated and equiaxed grains with (111) and (101) textures directed along the shearing plane. The observed elongated and equiaxed regions in the microstructure are compatible with the previous study conducted on pure Al indicating both grain types in the TEM micrographs after one pass [11,14]. Continuous recrystallization may have resulted in small equiaxed grains. Recrystallized grains have been observed after large deformations at low or room temperatures in copper [15] and other FCC metals [14,15]. Referring to Fig. 2(c) and 2(g), some of small angle boundaries are converted into the high angle boundaries after two passes. Both equiaxed and elongated grains with textures (111) [001] are included in the microstructure. It can be attributed to the fact that the deformed grain shears on the two orthogonal planes in the opposite direction due to the samples' rotation for the 2nd pass. After the third TCAP pass, high-angle boundary misorientation is mainly observed in the microstructure, which turn more homogeneous within the area (Fig. 2(d) and (h)). Similar to pure Al (99.9%) [16], the grain size decreases as the number of passes increases in the early stages of the TCAP processing. However, the grain size is around 0.48 μm after the third passes in this less pure material.

Figure 3 shows the fractions of grain boundaries (as a percentage) schemed as a function of the boundary misorientation angle for the unprocessed and processed samples through different number of passes. In Fig. 3, the misorientation distribution displays two simultaneous evolution types. First, a nonstop rise in the occurrence of high-angle misorientation towards the value range of 50–60°. Second, a modest rise in misorientation values in the range of 15–25° because of the conversion of subgrains into grains. Once the misorientation reaches the higher-range distribution, the range increase stops.

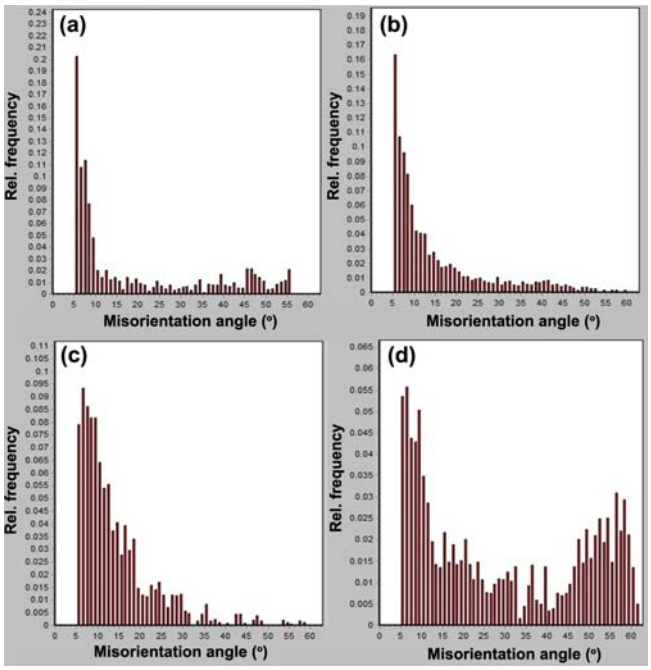

Fig. 3. Distributions of the boundary misorientation angle acquired from the EBSD information of (a) unprocessed and (b) 1 pass, (c) 2 passes, and (d) 3 passes processed samples.

However, a substantial portion of misorientation in the range of 15–25 continues primarily due to the conversion of sub-grains to grains, or a process of grain refining achieved its saturation limit [2,17]. It is clear from Fig. 3(d) that after 3 passes TCAP, the low angle grain boundaries are marginal. In fact, HAGBs surround the crystallites by their majority.

Figures 4(a)-(d) demonstrates the related histogram for grain size of the (a) 0 pass, (b) 1pass, (c) 2 pass and (d) 3 pass passes of the TCAP processed samples. Figure 4(a) displays the histogram alteration of grain size for 0 passes TCAP. It illustrates the actuarial variation of grain size, which gives an average size of around 75 μm. In the first pass (Fig. 4(b)), it is pellucid that the mean grain size is diminished from the preliminary grain size of 75 μm to an average cell size of 566 nm, which is in a good acquiescence with the antecedent work conducted on pure Al via (TCAP) [11]. Moreover, 9.88% of the grains are nanograins. The diameter of 0.325 μm has the maximum area fraction. As Fig. 4(c) illustrates, the maximum grain size, is 2.725 μm, and 15.73% of the grains have the diameter of nanometer range. The average grain size of about 500 nm is achieved for the 2 passes sample. The maximum considerable diameter of grains in 3 passes processed sample (Fig. 4(d)) is about 0.825 μm and the average grain size in this step is about 480 nm. This result is consistent with the quantitative EBSD result attained in former works [18-20]. The TEM was used combined with the EBSD having the TSL set up to warrant the accuracy and identify the right scanning parameters [15]. A grain tolerance of 5° was implemented and established that the size of the grain, as expected from the EBSD data, was greater than the real measured value in the TEM. That justifies the tolerance angle of 2° was implemented in the current work. When the crystalline materials are subjected to plastic deformation, the grains tend to align in certain crystallographic orientations with respect to the overall geometry of the sample. The tendency of the grains to be distributed at particular orientations is known as the texture of material. The texture controls the formability of crystalline materials, hence understanding the texture evolution is important. Figure 5 presents the pole figures of the unprocessed and TCAP processed tubes acquired using the EBSD technique in a particular position shown in Fig. 6. It is clear that the processing route leads to the shear texture. The intensity of texture rose as the number of passes increase.

The (111), (101) and (100) pole figures of the initial sample is shown in Fig. 5(a). It can be seen that the initial material has a strong cube texture. The measured (111), (101) and (100) pole figures for 1, 2 and 3 pass TCAP processed tubes in the axial direction of the sample were shown in Figs. 5(b)-5(d). Remarkable changes in texture can be observed after only one pass TCAP. It can be seen that the intensities of the texture increase from the first to the third pass. The overall

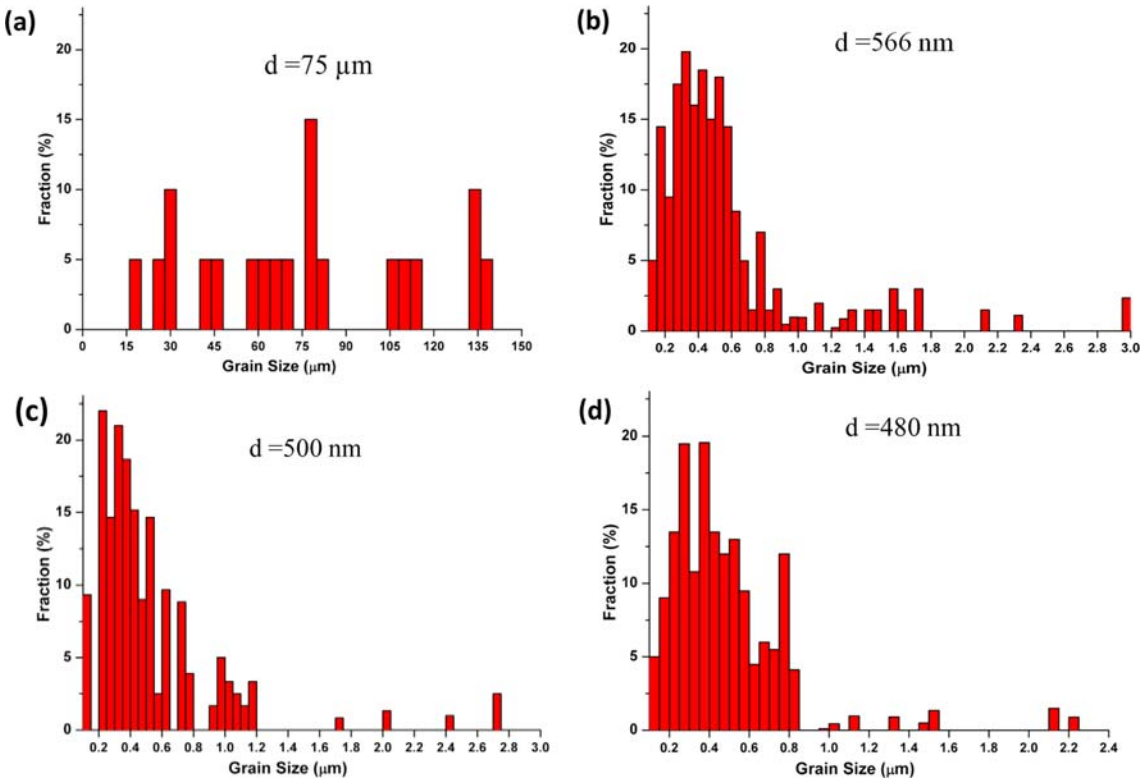

Fig. 4. Grain diameter distributions (from EBSD) for (a) 0 pass, (b) one pass, (c) two passes, and (d) three passes.

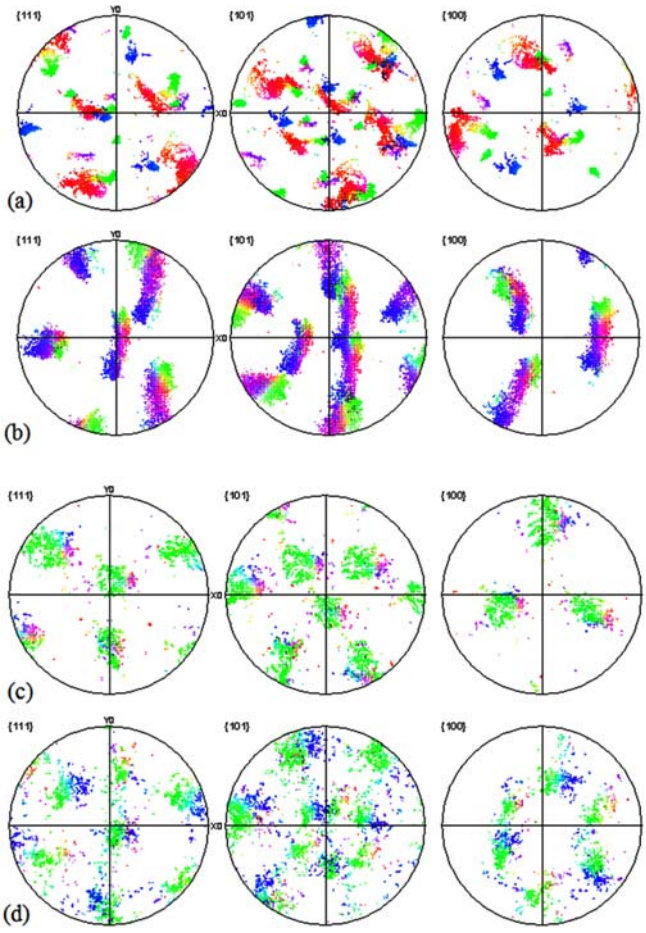

Fig. 5. EBSD pole figures acquired from the center region of the TCAP samples subjected to (a) zero, (b) one, (c) two, and (d) three passes.

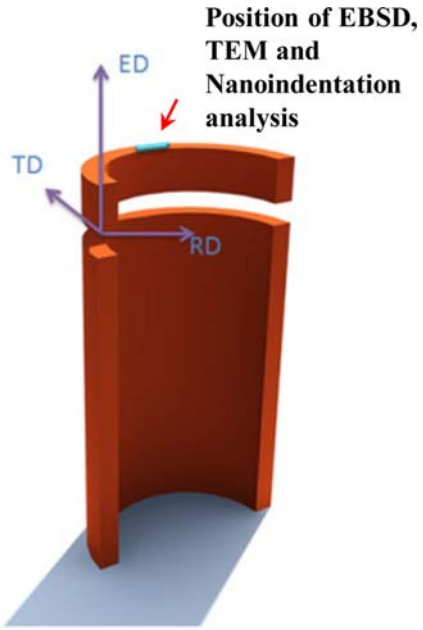

Fig. 6. Schematic drawing of the tube coordinates system and position of the measured element by EBSD analysis.

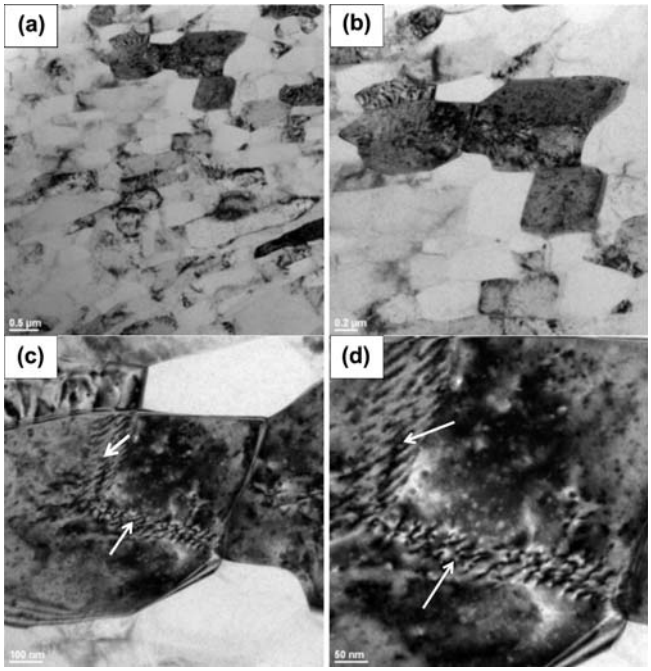

Fig. 7. TEM micrograph of the processed samples demonstrating (a) equiaxed fine grains, (b) subgrain boundaries inward the grains, (c) dislocations piled up to form subgrain boundary, and (d) higher magnification of dislocations in subgrain boundary (shown by arrow).

intensity of the third pass is stronger than just one pass. It can be concluded from the pole figures that the textures of 1 pass and three passes are close to ideal while the deviation from the ideal texture is obvious for two passes.

In Fig. 7(a), the TEM micrograph shows equiaxed and fine grain microstructure with distinct grain boundaries. Within most of the grains, the dislocation substructures were seen. As shown in Fig. 7(b), the grains were divided into subgrains by the subgrain boundaries. As shown in Fig. 7(c), these boundaries included a series of dislocations loaded on a particular plane. Dynamic recovery (DRV) happens in Al as a result of high stacking fault energy that resulted in the organization of dislocations into low-angle (2–5° misorientation) subgrain boundaries. Dislocations created while the TCAP deformations are absorbed in the subgrain boundaries and the misorientation increases to convert them into low-angle grain boundaries (5–15°). In Fig. 7(d), the greater magnification of the dislocations in the subgrain boundary is evident. A continuous dynamic process of recrystallization turns these low angle boundaries into high angle boundaries, resulting in the fine-grained structure [6]. Some fine precipitates can also be seen in the TEM images, which are rich in magnesium, silicon and iron as common aluminum impurities. These can also be seen in the base metal.

Indentation load-displacement curves were measured at four samples; zero passes, first pass, second pass and third pass and they are displayed in Fig. 8. These curves plainly

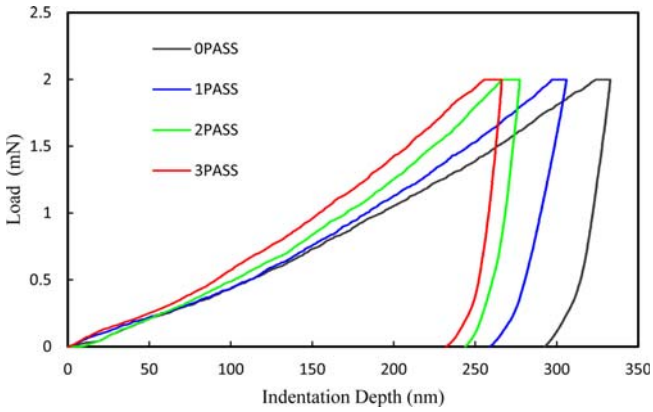

Fig. 8. Indentation load-displacement curve during zero, first, second and third pass of TCAP.

demonstrate that the final indentation depth decreases on the TCAP processed material via different passes compared to the unprocessed sample. This indicates that the work hardening rate is smaller in the processed samples in comparison with the unprocessed sample. The hardness values from the P-h curve of Fig. 8 are estimated using the so-called Oliver-Pharr method. The hardness values of 0.83 GPa, 1.05 GPa, 1.21 GPa and 1.3 GPa are obtained for the 0P, 1P, 2P and 3P processed samples. On the other hand, the TCAP processed samples show increased hardness compared to the unprocessed sample. Apart from that, the hardness enhancement in the first pass is maximum compared to the next passes.

Young's modulus is one of the mechanical properties which can be acquired from the load-displacement information of the Nano indentation test. It is ascertained through the use of the Sneddon relationship [1] as:

$$\frac{1}{E_r} = \frac{1-\nu^2}{E} - \frac{1-\nu_i^2}{E_i} \tag{2}$$

where E and E_i are Young's modulus of the test sample and indenter tip correspondingly, whereas ν and ν_i are Poisson's ratio of the test sample and indenter tip respectively. E_r is the reduced elasticity modulus of the material which is gained from the Nano-indentation test based on the Oliver-Pharr's method [21]. For calculating the Young's modulus of the Al samples, the values of ν = 0.33, and ν_i = 0.07 and E_i = 1140 GPa were considered in Eq. (2). The values used for ν_i and E_i are taking into account the technical data accessible for the related Triboindenter system. Figure 9 shows that the Module of elasticity of TCAP processed samples is greater from that of an unprocessed one. In addition, an increase in the TCAP passes prompts an increment in the module of elasticity. This could be considered an important feature of SPD processed materials.

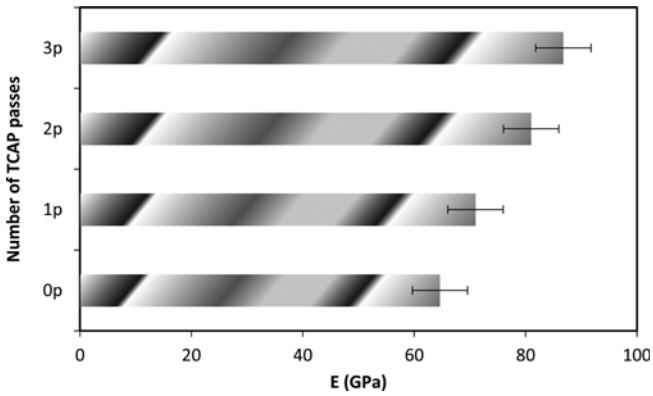

Fig. 9. The Module of elasticity of an unprocessed and TCAP processed sample.

4. CONCLUSIONS

In this current study, pure Al 1060 tubes were subjected to severe plastic deformation at room temperature by TCAP. The effect of the number of passes on the microstructure and mechanical properties were investigated using EBSD, TEM and nanoindentation analysis. Following conclusions could be made:

Severe plastic deformation induced by TCAP can produce substantial grain refinement.

(1) The increase in the strain of TCAP process increases the grain refinement rate in the tube because of the microstructural and textural mechanisms.

(2) The fraction of high-angle boundaries and average angle of boundary misorientation increase quickly up to 3 passes.

(3) By increasing the number of TCAP passes, the mean grain size of the processed materials lessened.

(4) Even after three passes, the TEM analysis exhibited a somewhat large amount of small angle boundaries with a misorientation angle under 2, so these were not involved in the EBSD analysis because of the limited angular resolution of the EBSD.

(5) Nanoindentation results revealed high module of elasticity and hardness for SPD processed samples compared to the unprocessed one.

(6) An increase of TCAP passes leads to a rise in the module of elasticity and hardness.

ACKNOWLEDGMENT

The authors would like to acknowledge the University of Malaya for providing the necessary facilities and resources for this research. This research was fully funded by the Ministry of Higher Education and also Ministry of Science, Technology and Innovation, Malaysia with the high impact research (HIR) grant number of UM.C/625/1/HIR/MOHE/ENG/27 and the e-Science Fund grant number of 03-01-03-SF0788 respectively.

REFERENCES

1. Y. T. Zhu, T. C. Lowe, and T. G. Langdon, *Scripta Mater.* **51**, 825 (2004).
2. M. Kawasaki, Z. Horita, and T. G. Langdon, *Mater. Sci. Eng. A* **524**, 143 (2009).
3. Y. Ito and Z. Horita, *Mater. Sci. Eng. A* **503**, 32 (2009).
4. M. Reihanian, R. Ebrahimi, N. Tsuji, and M. Moshksar, *Mater. Sci. Eng. A* **473**, 189 (2008).
5. A. Babaei, G. Faraji, M. Mashhadi, and M. Hamdi, *Mater. Sci. Eng. A* **558**, 150 (2012).
6. D. Yadav and R. Bauri, *Mater. Sci. Eng. A* **539**, 85 (2012).
7. M. Arzaghi, J. Fundenberger, L. Toth, R. Arruffat, L. Faure, B. Beausir, and X. Sauvage, *Acta Mater.* **60**, 4393 (2012).
8. G. Faraji, M. M. Mashhadi, and H. S. Kim, *Mater. Lett.* **65**, 3009 (2011).
9. A. S. Mohammadi, M. M. Mashhadi, and G. Faraji, *Modares Mech. Eng.* **15**, 126 (2015).
10. G. Faraji, P. Yavari, S. Aghdamifar, and M. M. Mashhadi, *J. Mater. Sci. Technol.* **30**, 134 (2014).
11. M. Mesbah, G. Faraji, and A. Bushroa, *Mater. Sci. Eng. A* **590**, 289 (2014).
12. G. Faraji, M. M. Mashhadi, S.-H. Joo, and H. S. Kim, *Rev. Adv. Mater. Sci.* **31**, 12 (2012).
13. A. J. Schwartz, M. Kumar, B. L. Adams, and D. P. Field, *Electron Backscatter Diffraction in Materials Science*, pp.263-266, Springer (2009).
14. C. Xu, M. Furukawa, Z. Horita, and T. G. Langdon, *Acta Mater.* **51**, 6139 (2003).
15. A. Mishra, B. Kad, F. Gregori, and M. Meyers, *Acta Mater.* **55**, 13 (2007).
16. J.-Y. Chang, J.-S. Yoon, and G.-H. Kim, *Scripta Mater.* **45**, 347 (2001).
17. M. Cabibbo, E. Evangelista, and C. Scalabroni, *Micron*, **36**, 401 (2005).
18. M. Reihanian, R. Ebrahimi, M. Moshksar, D. Terada, and N. Tsuji, *Mater. Charact.* **59**, 1312 (2008).
19. M. Mohebbi and A. Akbarzadeh, *Mater. Sci. Eng. A* **528**, 180 (2010).
20. I. Sabirov, M. Y. Murashkin, and R. Valiev, *Mater. Sci. Eng. A* **560**, 1 (2013).
21. W. C. Oliver and G. M. Pharr, *J. Mater. Res.* **19**, 3 (2004).